Calibration of ophthalmic applicators at NIST: A revised approach

C. G. Soares
National Institute of Standards and Technology, Gaithersburg, Maryland 20899

(Received 8 November 1990; accepted for publication 25 January 1991)

A revised approach to the problem of measuring a surface-absorbed dose from beta-particle-emitting ophthalmic applicators is presented. The technique chosen employs an extrapolation chamber equipped with a 4-mm-diam collecting electrode to make current measurements at air gaps from 0.08 to 0.20 mm at 0.02-mm intervals. These data yield a linear relationship between current and air gap, the slope of which is used to determine average surface-absorbed-dose rate over the central area of the source. For additional information about the distribution of the activity over the source surface, autoradiographs using calibrated radiochromic dye films are analyzed to map the dose-rate profile across the surface of the applicator. Experiments varying several parameters of the extrapolation chamber measurement, including collecting electrode area, voltage gradient, range of air gaps used, and entrance foil material, are described. Also treated are calibrations of, and a description of the use of, radiochromic dye films for source profiling. Experiments for determining correction factors for the extrapolation chamber measurements are described, and an assessment of the uncertainties associated with these measurements is given.

I. INTRODUCTION

The National Institute of Standards and Technology (NIST) has offered a service for the calibration of $^{90}Sr + {}^{90}Y$ beta-particle-emitting ophthalmic applicators since 1978.[1] Between then and June 1989, approximately 60 sources were calibrated in terms of surface-absorbed-dose rate to water. In 1988 a 38% discrepancy was observed in calibrations of the same source by NIST and Amersham International, currently the only manufacturer of ophthalmic applicators.[2] Amersham has been making and calibrating such sources since the 1950s. For the source in question (S/N 0625ML), NIST reported a dose rate of 0.73 Gy/s, while Amersham reported a dose rate of 0.45 Gy/s. In March 1989 a multinational workshop was held at NIST to explore the reasons for this discrepancy. One of the results of this workshop was the initiation of a laboratory intercomparison of two sources. The decision was made at NIST in June 1989 to suspend source calibrations for the public until the reasons for the discrepancy had been thoroughly explored. In the meantime, other laboratories in the U.S. employing extrapolation chambers, radiochromic dye films, and thermoluminescence dosimeters have published results which appear to agree with the NIST calibrations.[3,4,5,6] Nevertheless, NIST embarked upon a series of tests to evaluate and refine its calibration technique and hopefully to resolve the observed discrepancies.

II. EXTRAPOLATION CHAMBER MEASUREMENTS

A. Electrode size and range of air gaps

Absorbed-dose rate to water at the source surface is determined from current measurements with an extrapolation ionization chamber. The dose rate $\dot{D}$ is calculated from

$$\dot{D} = \frac{(\overline{W}/e) S_a^w B U}{\rho_{air} A} \left(\frac{\Delta I}{\Delta d}\right)_0, \quad (1)$$

where $(\Delta I/\Delta d)_0$ is the rate of change of current (normalized to reference conditions of 22° air temperature and 101.3 kPa air pressure) with extrapolation chamber air-gap thickness as the thickness approaches zero, $(\overline{W}/e)$ is the mean energy required to produce an ion pair in dry air divided by the elementary charge (taken to be 33.97 J/C), S_a^w is the ratio of the mean mass stopping power of water to that of air (taken to be 1.12), ρ_{air} is the density of air at the reference conditions (1.197 kg/m^3), B is a correction for reduced backscatter from the graphite collecting electrode relative to that of water (taken to be 1.005), U is a correction for attenuation by the high-voltage electrode [measured as 1.003 (Ref. 1)], and A is the effective ionization collection area. For an electrode which is smaller than the active area of the source, this is taken as the area corresponding to the radius of the collecting electrode itself plus one-half of the thickness of the insulating gap between the electrode and guard ring. These distances were measured for all the electrodes used in the experiments using a traveling microscope. The source center is determined by mapping the relative dose rate across the source surface with a 1-mm-diam collecting electrode in a manner identical to that formerly used in this laboratory to measure source areas.

The original calibration procedure employed a 28-mm-diam tissue-equivalent plastic electrode to measure the average absorbed-dose rate over the entire area of the source. For this measurement, the effective collection area was taken as the active area of the source, defined as the area within the 50% isodose line at the source surface and measured by mapping the relative dose rate across the source surface with the 1-mm-diam collecting electrode. This method of specifying the absorbed-dose rate suffers from the flaw that ionization is measured over the entire 28-mm-diam area, arising in part from beta particles being emitted from the source edges and areas beyond the 50% isodose area, while the area that the dose is assumed to arise from is fixed at the 50% isodose

area. Depending on the steepness of the shoulders of the radial dose-rate profile, this method yields a dose rate that is larger than the maximum dose rate at the source center.

In the past, air gaps of 0.5–2.5 mm in 0.5-mm steps were used; a cubic polynomial was fitted to the current–versus–air-gap data, and this function was forced through zero. However, this procedure caused difficulties because of apparent variations in the collecting electrode dimensions, which caused a change in the location of the zero air-gap setting.[7] To overcome this problem, a quadratic function was used for an initial fit to determine the location of the intercept, which then allowed one to correct the air gaps; the data were then refitted using the corrected air gaps with a quadratic function forced through zero; the slope at zero air gap was then determined. Air-gap corrections were generally on the order of $\pm$ 10 μm. This change resulted in greatly improved reproducibility in the measured slope for the NIST-owned quality assurance source. This procedure was performed in calibrations done from December 1988 to June 1989 when the service was suspended. Also, calibrations performed between 1986 and 1988 were amended, and revised reports were issued. The revisions necessary to the NIST-measured dose rates were 5%–15% downward, depending on the date the original calibration was performed. The revised dose-rate estimate for S/N 0625 was 0.62 Gy/s, which reduced the discrepancy with Amersham to 27%.[4]

In an effort to explore possible reasons for the remaining discrepancy between NIST and Amersham International, a number of parameters of the extrapolation procedure were varied to assess the effect on the measured dose rate. The principal difference between the Amersham geometry[8] and that formerly used at NIST is the size of the collecting electrode (see Table I). The availability of a range of different size graphite electrodes at NIST allowed a study of measured dose rate as a function of this parameter. Initial measurements using extrapolations of air-gap measurements between 0.5 and 2.5 mm indicated that there was indeed an apparent strong dependence of the measured dose rate on the collecting electrode area used. However, when measurements were repeated at smaller air gaps, between 0.1 and 0.5 mm, it was found that the previous measurements were in error because of the increasing curvature of the current–versus–air-gap function at greater than 0.2-mm air gaps. For this reason, all measurements were henceforth made at the smaller air gaps. In addition, the 4-mm-diam graphite electrode was adopted for subsequent dose-rate determinations. This selection was based upon the availability of this electrode and represents a compromise, since, ideally, a very-small-area electrode should be used which would measure true maximum absorbed-dose rate; however, such a measurement would suffer from having a larger systematic error in the measurement of collection area.

Further investigations into the discrepancy indicated that there is a difference in the assumptions made as to the shape of the current–versus–air-gap function as zero air gap is approached. Inherent in the NIST quadratic model is the assumption of a continuously changing slope; Amersham (and others, notably Loevinger in 1953[9]) assumes that once one has found a linear region in the current–versus–air-gap function, this slope will continue to zero air gap. To test which assumption is valid, a special experiment was performed where the high-voltage electrode foil was removed and the source itself biased to form the high-voltage electrode. It was found that indeed there is a linear region, from 0.2 down to about 0.06 mm. Figure 1 shows these data, taken at 0.02-mm intervals, along with data taken at 0.1-mm intervals to 0.5

TABLE I. Modifications in NIST technique and comparison to Amersham International technique.

Extrapolation chamber geometry	Former NIST	Revised NIST	Amersham
Collecting electrode	28-mm diam tissue-eq. plas.	4-mm diam graphite	3-mm C-coated tissue-eq. plastic
Window foil	single-sided Al-Mylar 0.9 mg/cm^2	same	double-sided Al-Mylar 1 mg/cm^2
Range of air gaps	0.5–2.5 mm	0.08–0.2 mm	0.1–0.25 mm
Voltage gradient	20 V/mm	100 V/mm	100 V/mm
Recombination	from theory	from exper.	none
Source potential	grounded or floating	at foil potential	at foil potential
Added absorbers	none	none	6-mg/cm^2 plas.
Depth of quoted measurement	surface	surface	7 mg/cm^2
Medium of quoted measurement	water	water	tissue
Fit function used for extrapolation	quadratic	linear	linear
Constants used for dose-rate calculation			
$\overline{W}/e$	33.7 J/C	33.97 J/C	32.5 J/C
Ratio of stopping powers rel. to air	1.124 water	1.12 water	1.11 tissue
Backscatter of electrode rel. to medium	1.010	1.005	1
Half-life	28.50 y	28.50 y	28.6 y

mm. The data at 0.2 mm and below yield a well-defined linear function, which has the advantage that the slope at zero air gap is independent of the exact location of zero air gap. This is further illustrated in Fig. 2, which shows the same data, but this time transformed to show current per unit air gap versus air gap. The horizontal solid line is the slope as determined from a least-squares fit of the data between 0.6 and 0.2 mm, while the dashed line is the quadratic fit of the 0.1- to 0.5-mm data with air gaps adjusted (in this case by 2 μm), as described in an earlier paragraph. Because of the sensitivity of the quadratic model on the exact location of zero air gap (which cannot be determined to very great precision), the NIST procedure was further modified to make current measurements from 0.08 to 0.2 mm at intervals of 0.02 mm. As shown in Fig. 2, this modification in technique reduces the NIST-measured slopes by an additional 10% over the interim method based on quadratic fitting of 0.1–0.5-mm air-gap measurements. The linear relationship breaks down at air gaps less than about 0.05 mm, possibly as a result of interface effects.[10] The presence of the 0.2-mm-thick insulating gap between the collecting electrode and guard ring may also cause the linear relationship to break down because of the perturbation of the electric field at the very smallest air gaps.

B. Recombination correction

An investigation of the recombination correction used previously[1,11] was made when it was found that it seriously underestimated the corrections necessary for small air gaps, especially at the previously used gradient of 20 V/mm. In this region, the correction for loss of ions due to diffusion against the polarizing field onto the collecting electrode predominates. The correction traditionally used comes from the theory of Langevin.[12] Measurements of net collected current were made as a function of voltage gradient from 20 to 500 V/mm. These measurements could only be made successfully when the source was kept at the same potential as the high-voltage foil electrode; grounding the source as was done previously causes the foil to be pulled toward the source at the higher voltages, giving erroneous currents due to increased collection volume. Once this change was made, currents could be measured without foil deformation at voltage gradients up to 400 V/mm; at higher gradients, the foil was pulled toward the grounded collecting electrode, thus reducing the measured currents. The saturation current was determined by plotting the currents versus the inverse of the square root of the applied voltage.[9] This transformation yields a straight line for voltage gradients between 100 and 400 V/mm, where the electrostatic attraction between the foil and collecting electrode is minimal. This line can then be extrapolated to zero (infinite voltage) to yield the saturation current. The resulting determinations of the recombination correction for the 4-mm electrode are shown in Table II. They were found to agree well with those of Loevinger's empirical function[13]

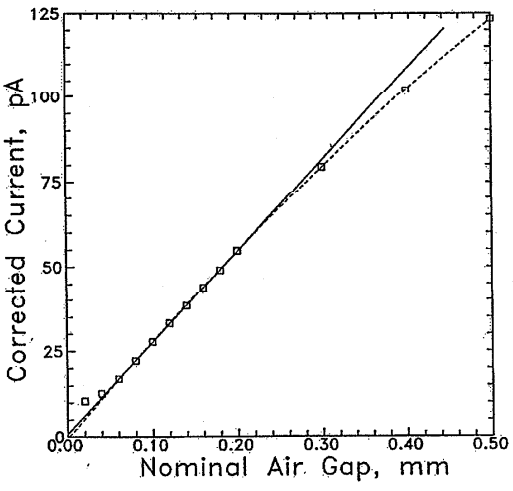

FIG. 1. Extrapolation chamber data taken with a 4-mm-diam collecting electrode. Boxes: measured points; solid line: linear least-squares fit to the data between 0.06 and 0.20 mm; dashed line: quadratic least-squares fit to the 0.1- and 0.2–0.5-mm data points.

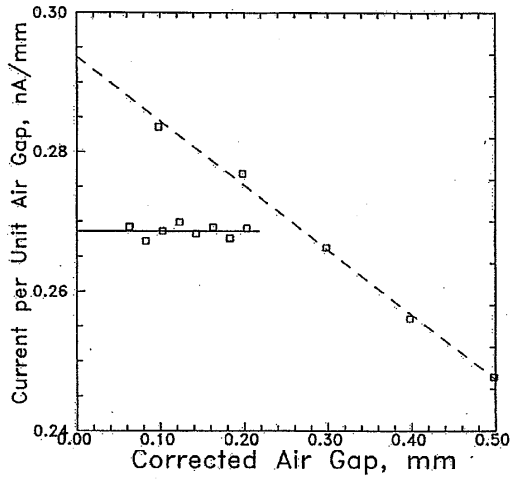

FIG. 2. The same extrapolation chamber data as shown in Fig. 1, but transformed to show current per unit air gap versus corrected air gap. Solid line: slope of the least-squares fit shown in Fig. 1, with the air gaps for the data along this line corrected by 3.02 μm, which is the x intercept of the linear least-squares fit shown in Fig. 1; dashed line: least-squares fit of the 0.1- and 0.2–0.5-mm data whose air gaps were corrected by -2.02 μm, which is the x intercept of the quadratic fit shown in Fig. 1. The y intercepts of these two lines represent the slope at zero air gap for the two models (linear and quadratic) considered in the text.

TABLE II. Measured recombination corrections.

Air gap (mm)	Voltage gradient (V/mm) 20	100	200	300	400
0.1	1.093	1.043	1.030	1.025	1.024
0.2	1.042	1.022	1.015	1.012	1.011
0.3	1.031	1.016	1.012	1.009	1.008
0.4	1.024	1.013	1.009	1.007	1.006
0.5	1.021	1.011	1.008	1.006	1.005

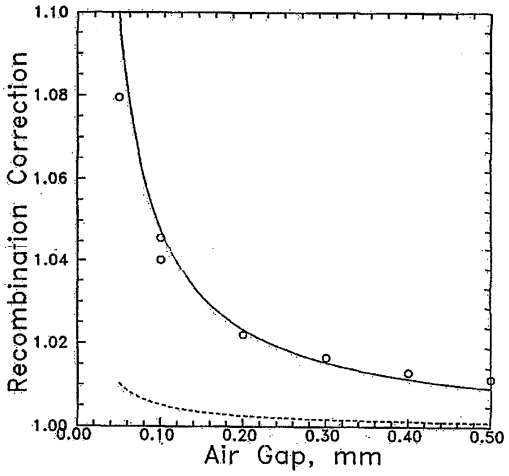

FIG. 3. Small-air-gap recombination corrections for 100-V/mm voltage gradient. Circles: this experiment; solid line: predictions of Loevinger's empirical relation (Refs. 9 and 13); dashed line: predictions of Langevin's theory (Refs. 11 and 12).

$$I_0/I_\infty = 1 - 0.0144/(Vd)^{1/2}, \quad (2)$$

where d is in cm. As shown in Fig. 3 for the 100-V/mm corrections, there does appear to be some trend with air gap not accounted for in this function. An interesting result of this measurement is that the necessary corrections do not affect the measured slope of the current–versus–air-gap function since it was found that the product of the correction and the corresponding air gap is nearly constant. Since the current–versus–air-gap function is linear, the corrections have only the effect of changing the zero intercept of the function by this product (approximately 4 μm), which is apparently the distance from the collecting electrode at which the diffusion effect occurs.

C. High-voltage electrode material and thickness

Another difference between the two laboratories is the thickness of the high-voltage electrode and the depth at which the measurement is quoted. To assess the effect of this difference, measurements were made of slope (measured between 0.08 and 0.20 mm) as a function of window material and thickness. Five high-voltage electrode configurations were investigated, all measured with the 4-mm-diam graphite electrode operated at a constant-voltage gradient of 100 V/mm with the experimentally determined recombination corrections applied. The configurations investigated were (1) no entrance foil (mentioned above), (2) the normal single-sided aluminized Mylar used at NIST, (3) double-sided aluminized Mylar obtained from Amersham, (4) single-sided aluminized Mylar to which was added 6 mg/cm^2 of polyester, and (5) double-sided aluminized Mylar to which was added the same piece of polyester as in (4). Two measurements were made at each configuration and the results (which differed from each other by no more than 1.3%) averaged. Table III contains the results, shown relative to the no-foil slope. As indicated in the table, the current NIST correction for the presence of the high-voltage electrode may be about 0.5% low. These results indicate that the Amersham calibration data need a correction of about 7% to make them comparable to the NIST values, which are quoted for the source surface.

TABLE III. Effect of high-voltage electrode material on measured dose rate.

Configuration	Thickness (mg/cm^2)	Relative dose rate[a]
No foil	0	1.000
Single-sided Al Mylar	0.9	0.993
Double-sided Al Mylar	1.0	0.967
Single-sided Al Mylar + 6.2 mg/cm^2 polyester	7.1	0.941
Double-sided Al Mylar + 6.2 mg/cm^2 polyester	7.2	0.933

[a] Results are the average of two measurem[illegible], shown relative to the "no foil" configuration.

III. DYE FILM MEASUREMENTS

A. System description

Radiochromic dye films[14,15] (GafChromic), consisting of a thin sensitive coating (6–7 μm) on a nominal 100-μm (0.004-in.) Mylar base, were used to map dose-rate variations at applicator surfaces. (In this paper, certain commercially available products are referred to by name. These references are for information purposes only and do not imply that these products are the best or only products available for the purpose, and do not imply endorsement by NIST.) These films require no processing and can be exposed to normal room lighting; they turn blue on exposure to ionizing radiation at dose levels above about 100 Gy. The films were read using a scanning laser densitometer (LKB Pharmacia model 2222-020) at 633 nm, which is near one of the peaks of the film absorbance spectrum. The spot size of the laser is 100 μm in diameter, and the step size for scanning is adjustable in 40-μm increments in both dimensions. The accuracy of the stepping increment was checked by scanning a microscope stage micrometer and a NIST glass scale. The absolute linear accuracy of the system was found to be accurate to less than 1 μm. The same scales were also used to check the linear accuracy of the traveling microscope that was used for measuring collecting electrode areas.

B. Calibration

Use of the dye film for measurement of dose requires that it be calibrated. Usually this is accomplished using well-characterized ^{60}Co gamma-ray beams. There is some question, however, as to how well this calibration predicts film response when electron irradiations are used. To check this, calibrations were performed using both ^{60}Co gamma rays and ^{90}Y beta particles. The latter was done using the protection-level sources used at NIST for instrument and source calibrations. There is agreement between NIST and the Physikalisch–Technische Bundesanstalt (PTB) on the dose rate from these sources at the prescribed distances.[16] Film was

irradiated at the 11-cm distance with the 50-mCi $^{90}Sr + ^{90}Y$ source to give a relationship between ^{90}Y beta-particle dose and film absorbance. Because of the relatively low dose rate of the source employed, a single exposure of 20 days was made. The shape of the dose-absorbance curve for broad-spectrum electrons was determined using surface exposures on an $^{90}Sr + ^{90}Y$ beta-particle ophthalmic applicator. This curve was then made absolute using the result of the known dose exposure from the protection-level source. The resulting dose-absorbance curve was found to be nearly the same as that obtained using a ^{60}Co gamma-ray calibration; however, at elevated dose levels (above around 700 Gy), the film appears to respond somewhat more to electrons than to ^{60}Co gamma rays. For the results presented here, the electron calibration was used.

C. Measurement procedure

For measurement of surface-absorbed-dose rate from ophthalmic applicators, 2×2-cm pieces of film were taped to a dummy tissue-equivalent plastic electrode, which was then placed in the extrapolation chamber for exposure. The resulting exposure geometry was thus nearly identical to that used for the extrapolation chamber measurements. Exposure times were on the order of a half hour. As reported elsewhere,[14] it was found that the radiation-induced image exhibits short-term instability: The color continues to develop after irradiation ceases. This effect makes it necessary to wait at least 1 day after irradiation before readout if accurate dosimetry is the object. For this work, it was found that after a 3-day delay the image stabilized and remained stable subsequently out to at least 1 month, the longest period that was tested.

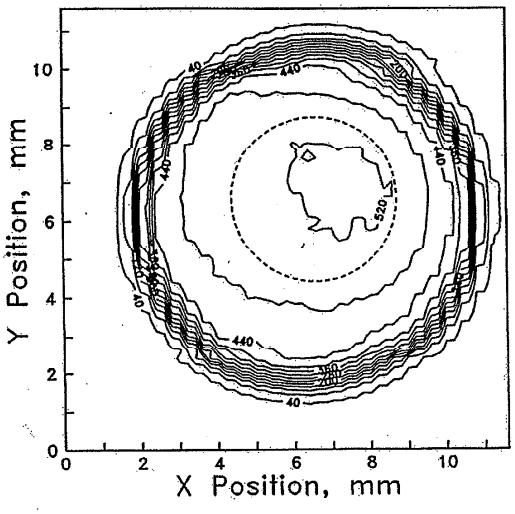

FIG. 4. Isodose-rate contour plot from a radiochromic-dye film autoradiograph of ophthalmic applicator S/N 0258. The contour intervals are 40 mGy/s and the dashed line represents the area averaged over when measurements are made with the extrapolation chamber equipped with a 4-mm-diam collecting electrode.

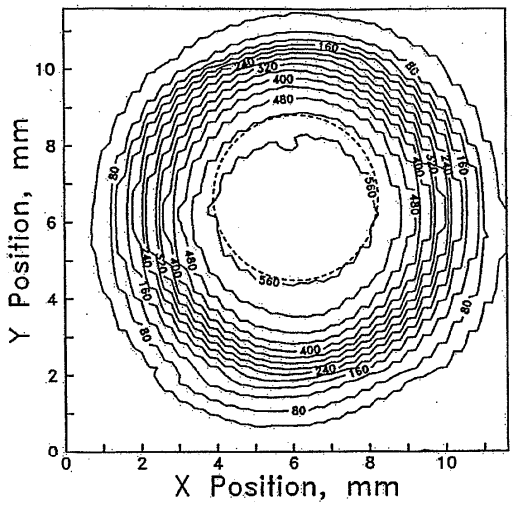

FIG. 5. Isodose-rate contour plot from a radiochromic-dye film autoradiograph of ophthalmic applicator S/N 0802ML.

The irradiated films were read using a full two-dimensional scan at a step size of 0.2 mm in each dimension over an area of 12 × 12 mm, which produces 3600 density measurements. The absorbance readings were then converted to dose rate using the calibration curve and the known exposure time. Using appropriate software, it is possible to generate isodose-rate profiles of the results of the scans. Examples of such plots are shown in Figs. 4–6. The dashed line on these plots represents the area averaged over when measurements are made with the extrapolation chamber equipped with a 4-mm-diam collecting electrode.

Currently it is difficult to perform absolute dosimetry using dye films because of the variability in film response. This

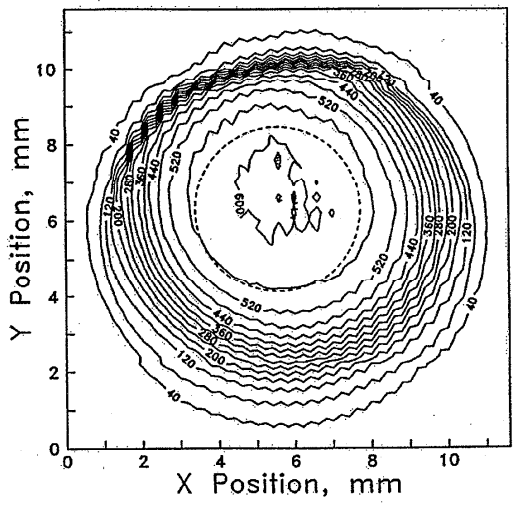

FIG. 6. Isodose-rate contour plot from a radiochromic-dye film autoradiograph of ophthalmic applicator S/N 0815ML.

TABLE IV. Estimated uncertainties in NIST calibration using the extrapolation chamber.

Component	Uncertainty (%)
Instrumental	0.3
Average energy per ion pair	0.4
Stopping-power ratio	3
Rate of change of current $(\Delta I/\Delta d)_0$	3
Backscatter correction B	1
Attenuation correction U	<0.1
Electrode area A	4
Combined uncertainty (quadratic sum)	6
Overall uncertainty (combined ×2)	12

is mainly due to variations in the thickness in the sensitive layer of individual films. Work is underway to overcome this problem, and a subsequent investigation is planned to address a comparison between results of dye film and extrapolation chamber measurements as a function of collecting electrode size.

IV. ASSESSMENT OF UNCERTAINTIES

The overall uncertainty of the NIST calibration procedure is estimated to be ± 12% (see Table IV). The random uncertainty components are calculated as standard deviations of the mean of replicate readings; other components are estimated so that they can be assumed to have the approximate character of standard deviations. The overall uncertainty is two times the square root of the quadratic sum of all the component uncertainties; it is considered to have the approximate significance of a 95% confidence limit.

V. COMPARISON OF FORMER AND PRESENT NIST CALIBRATION RESULTS

Because of the change in the collecting electrode made in the NIST calibration procedure, it is difficult to predict the change in measured dose rate between the two calibration methods for any given source. At present, measurements in both geometries have been performed on only three sources; the results are shown in Table V. As mentioned earlier, the difference is a function of the steepness of the dose-rate gradient at the source edges. Sources with sharp edges, such as S/N 0258 (Fig. 4) exhibit little change because the source area is well defined and essentially all within the 50% isodose contour. Sources with more gradual shoulders, such as S/N 0802ML (Fig. 5) exhibit somewhat more difference because of the significant contribution to ionization made by activity lying outside of the 50% isodose contour. Most sources will lie somewhere in between, such as S/N 0815ML (Fig. 6). We expect that, for nearly all sources previously calibrated at NIST, the change in dose rate will be downward by 10% or less.

TABLE V. Comparison of results between former and revised NIST calibration methods.

Source S/N	Absorbed-dose rate (Gy/s) Former NIST	Revised NIST	Ratio
0258	0.521	0.515	1.01
0802ML	0.637	0.584	1.09
0815ML	0.615	0.587	1.05

In addition to the physical changes in the calibration procedure, the constants used to calculate the absorbed-dose rate were reevaluated. The value for $\bar{W}/e$ was updated to 33.97 J/C to reflect the most recent international recommendations.[17] The stopping-power ratio of water relative to air was calculated by weighting stopping-power data[18] with a measure spectrum from an applicatorlike source.[16] The spectrum used was taken at a distance of 11 cm in air from the source and is assumed to be nearly equal to that at the source surface. Finally, the deficiency in electron backscatter from carbon relative to water was estimated using the empirical formula of Tabata *et al.*[19] These were averaged over the spectrum referred to above. The changes made are shown in Table I.

VI. CONCLUSIONS

Table I summarizes both the modifications made at NIST and the present differences between Amersham and NIST calibration procedures. At the time of writing, the Amersham method yields a calibration that is about 21% lower than the NIST method. If the NIST constants are used, and the Amersham calibration is corrected with the transmission factor between surface and 7 mg/cm^2 (measured as 0.93 in this laboratory), the discrepancy is reduced to about 10%. Given the quoted uncertainties in the respective calibrations, the agreement is satisfactory.

ACKNOWLEDGMENTS

The author would like to acknowledge the services and advice of the following NIST scientists: J. S. Pruitt for providing my introduction and instruction into this very tricky field, R. Loevinger for many helpful discussions concerning the historical and philosophical aspects of extrapolation chamber measurements, and B. M. Coursey for sympathetic and supportive leadership during this rather trying period. Crucial to the radiochromic dye film measurements are NIST scientists W. L. McLaughlin, our in-house dye-film expert, M. L. Walker, who introduced me to high-resolution laser densitometry, and J. M. Puhl, who assisted with the plotting software. S. J. Goetsch of UCLA Medical Center deserves credit for first bringing the discrepancy to light and for continuing interest in the project, and I thank J. A. Sayeg of the University of Kentucky for many useful discussions concerning the dye-film measurements. Finally, the largest debt is owed to J. O. Deasy, a graduate student currently doing research at the Brown Cancer Center at the University of Louisville, whose enthusiasm and interest in this problem has stimulated the initiation of many of the experiments performed.

[1] J. S. Pruitt, "Calibration of beta-particle-emitting ophthalmic applicators," NBS Special Publication 250-9 (July 1987).

[2] S. J. Goetsch, "Calibration of Sr-90 ophthalmic applicators" Int. J. Radiat. Oncol. Biol. Phys. **16**, 1653 (1989).
[3] M. M. Ali and F. M. Khan, "Determination of surface dose rate from a ^{90}Sr ophthalmic applicator," Med. Phys. **17**, 416–421 (1990).
[4] C. S. Reft, F. T. Kuchnir, I. Rosenberg, and L. C. Myrianthopoulos, "Dosimetry of Sr-90 ophthalmic applicators," Med. Phys. **17**, 641–646 (1990).
[5] J. A. Sayeg and R. C. Gregory, "A new method for characterizing beta ray ophthalmic applicator sources," Med. Phys. **18**, 453–461 (1991).
[6] S. J. Goetsch and K. S. Sunderland, "Surface dose rate calibration of ^{90}Sr plane ophthalmic applicators," Med. Phys. **18**, 161–166 (1991).
[7] C. G. Soares, "Recent NIST measurements of extrapolation chamber air gap thicknesses," presentation at the NIST Workshop on the Calibration of Ophthalmic Applicators, National Institute of Standards & Technology, Gaithersburg, MD, 6–7 March 1989 (unpublished).
[8] A. Ainsworth, "The measurement of beta dose rates from ^{90}Sr surface and ophthalmic applicators," manuscript of presentation at the NIST Workshop on the Calibration of Ophthalmic Applicators, National Institute of Standards & Technology, Gaithersburg, MD, 6–7 March 1989 (unpublished).
[9] R. Loevinger, "Extrapolation chamber for the measurement of beta sources," Rev. Sci. Instrum. **24**, 907–914 (1953).
[10] J. O. Deasy and C. G. Soares, "Extrapolation chamber measurements of ophthalmic applicators" (in preparation).
[11] J. Böhm, "Saturation corrections for plane parallel ionization chambers," Phys. Med. Biol. **21**, 754–759 (1976).
[12] P. Langevin, "Mesure de la valence des ions dans les gaz," Radium **10**, 113–118 (1913).
[13] R. Loevinger and N. G. Trott, "Design and operation of an extrapolation chamber with removable electrodes," Int. J. Appl. Radiat. Isot. **17**, 103–111 (1966).
[14] M. C. Saylor, T. T. Tamargo, W. L. McLaughlin, H. M. Khan, D. F. Lewis, and R. D. Schenfele, "A thin film recording medium for use in food irradiation," Radiat. Phys. Chem. **31**, 529–536 (1988).
[15] W. L. McLaughlin, Y.-D. Chen, C. G. Soares, G. Van Dyk, and D. F. Lewis "Sensitometry of a new radiochromic film dosimeter response to gamma radiation and electron beams," Nucl. Instrum. Meth. Phys. Res. (to be published).
[16] J. S. Pruitt, C. G. Soares, and M. Ehrlich, "Calibration of beta-particle radiation instrumentation and sources," NBS Special Publication 250-21 (April 1988).
[17] Comité Consultatif pour les Étalons de Mesure des Rayonnement Ionisants, Rapport de la 11e session, R157, Bureau International de Poids et Mesures (1985); M. Boutillon and A. M. Perroche-Roux, "Re-evaluation of the W value for electrons in dry air," Phys. Med. Biol. **32**, 213–219 (1987).
[18] M. J. Berger and S. M. Seltzer, "Stopping powers and ranges of electrons and positrons," 2nd ed., Rep. NBSIR 82-2550-A (1983).
[19] T. Tabata, R. Ito, and S. Okabe, "An empirical equation for the backscattering coefficient of electrons," Nucl. Instrum. Meth. **94**, 509–513 (1971).